Intercalant-Induced Superbundle Formation of Single-Wall Carbon Nanotubes

Kay Hyeok An,[†,‡] Cheol-Min Yang,[‡] Jin Sung Park,[†] Seung Yol Jeong,[†] and Young Hee Lee*[,†,‡]

BK21 Physics Division, and Institute of Basic Science, Center for Nanotubes and Nanostructured Composites, Sungkyunkwan University, Suwon 440-746, Republic of Korea

Received: January 31, 2005; In Final Form: March 23, 2005

The formation of a massive quantity of single-wall carbon nanotube (SWCNT) superbundles has been introduced through sonicating SWCNTs in tetramethylene sulfone/chloroform solution in which nitronium hexafluoroantimonate (NHFA) is dissolved. Most SWCNT bundles with the NHFA treatment are enlarged by about 10 times compared with those of the pristine sample. It is proposed that the formation of SWCNTs can occur in solution by formation of an SWCNT−intercalant charge complex. The specific surface area of the superbundle is almost doubled, while its micropore surface area is amplified by about 7 times. This development of microporosity results from the enhanced interstitial sites in the SWCNT superbundles.

Introduction

Since the discovery of carbon nanotubes (CNTs) as a novel form of carbon, there have been numerous new applications using CNTs. In particular, CNTs have been suggested as a new candidate material for energy storage devices, such as hydrogen storage systems,[1,2] fuel cells,[3] lithium ion secondary batteries,[4] and supercapacitors[5,6] due to their low mass density, low resistivity, large surface area, and unique pore structures. The unique pore structures of CNTs originate from bundles that are formed by van der Waals interaction between individual CNTs. Recently, many researchers have reported that CNTs with large bundles showed excellent performance in hydrogen storage and lithium ion batteries.[7−10] Therefore, controlling the bundle structures is an essential step in improving the performance of energy storage devices.

Several groups reported that the purification of single-wall carbon nanotubes (SWCNTs) by acid treatment slightly enlarged the bundle sizes of SWCNTs.[11−14] It has been often observed that a small quantity of superbundles could be obtained from the supernatant on the water surface after a sonication process, while the majority of SWCNTs remaining in the precipitates revealed typical bundle sizes of less than 30 nm.[14] The bundle sizes were enlarged by an agglomeration of hydrophobic SWCNTs in a polar solvent (for instance, water and alcohol) such that van der Waals interaction was maximized between nanotubes. Formation of superbundles in a large quantity using a polar solvent has been hardly observed. Contrary to this, CNTs are easily wettable in aprotic solvents. One expects that CNTs can be well dispersed in aprotic solvents, and therefore the diameters of CNT bundles are expected to be relatively small in such a solvent.[14,15] No systematic studies have been developed yet to yield a mass quantity of the large bundles in aprotic solvents.

In this paper, we have introduced a simple and easily scalable method for the formation of a massive quantity of SWCNT superbundles by sonicating SWCNTs in tetramethylene sulfone (TMS)/chloroform solution in which nitronium hexafluoroantimonate (NO_2SbF_6; NHFA) was dissolved. This involved the intercalation of NHFA into bundles followed by a rearrangement of SWCNTs via the bridged intercalants to form superbundles. The bundle sizes were significantly enlarged to about 250 nm. The specific surface area of the superbundle was almost doubled, while its micropore surface area was amplified by about 7 times.

Experimental Section

NHFA of 10−40 mmol was dissolved in 100 mL of TMS/chloroform (1:1 by weight) solution. The pristine HiPCO SWCNT soot (10 mg) purchased from CNI (Carbon Nanotechnologies Inc.) was sonicated in the prepared NHFA solution for 6−48 h. After NHFA treatment, the suspension was filtered using a membrane filter with a pore diameter of 10 μm and then washed with ethanol and acetone several times. The residual SWCNTs on the filter were dried in a vacuum at 100 °C overnight. The morphology of the NHFA-treated SWCNTs was observed by use of a field-emission scanning electron microscope (FESEM; Hitachi S4700) at 15 kV accelerating voltage and a field-emission high-resolution transmission electron microscope (HRTEM; JEOL-JEM3011) at 200 kV accelerating voltage. X-ray photoemission spectroscopy (XPS) was carried out using a PHI 5100 spectrometer with the Mg Kα (1253.6 eV) line. The pore structures were determined by N_2 adsorption isotherm at 77 K using volumetric equipment (Micromeritics ASAP2020), after preevacuation at 473 K for 12 h, while maintaining the base pressure at 10^{-4} Pa. The parameters of the pore structures were obtained by the subtracting pore effect (SPE) and Brunauer−Emmett−Teller (BET) methods. The SPE method was performed by using high-resolution α_s-plots that were constructed for the standard adsorption data on highly crystalline nonporous carbon black. We introduced the Horvath−Kawazoe (HK) and Barrett−Joyner−Halenda (BJH) methods to determine the micropore and mesopore size distributions, respectively.

Results and Discussion

First, the pristine SWCNTs were sonicated in TMS/chloroform solution without NHFA to understand the sonication effect of the used solvents. Parts a and b of Figure 1 show the

* Corresponding author. E-mail: leeyoung@skku.edu.
† BK21 Physics Division.
‡ Institute of Basic Science.

10.1021/jp050544t CCC: $30.25
Published on Web 04/26/2005

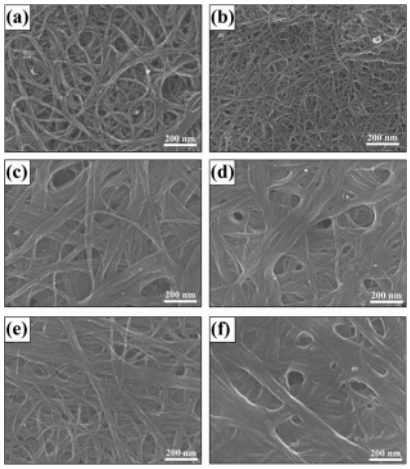

Figure 1. FESEM images of (a) pristine SWCNTs, (b) SWCNTs after sonication for 24 h in TMS/chloroform without NHFA, (c, d) SWCNTs after NHFA treatment for 24 h in (c) 10 and (d) 40 mmol, and (e, f) SWCNTs after NHFA treatment in 40 mmol for (e) 6 and (f) 48 h.

FESEM images of the pristine SWCNTs before and after sonication in TMS/chloroform solution without NHFA for 24 h. The bundles of the pristine SWCNTs were randomly entangled with a broad diameter distribution of 5−30 nm, as shown in Figure 1a. On the other hand, the bundles of the SWCNTs after sonication in TMS/chloroform solution were disrupted into small bundles with a uniform diameter distribution of 5−10 nm, as shown in Figure 1b. It has been well known that the polarity of the solvent greatly affects the size and density of the bundles after sonication.[14] Sonication in organic solvents such as toluene, dimethylformamide, tetrahydrofuran, and dichloroethane produces smaller bundle diameters than that it does in water and alcohols with large polarity.[14]

Parts c and d of Figure 1 show the FESEM images of NHFA-treated SWCNTs after sonication for 24 h as a function of the NHFA concentration. Large bundles, called "superbundles", were formed after sonication in NHFA solution, in good contrast to similar treatment without NHFA. The bundle sizes and the number of superbundles increased prominently with increasing NHFA concentration, and some of them reached the bundle size of about 250 nm. The bundle sizes were saturated at 40 mmol of NHFA. The influence of the sonication time in NHFA solution is also presented in Figure 1e,f. The small bundles were agglomerated further with increasing sonication time and saturated to superbundles with diameters of about 250 nm after 24 h. We emphasize that the NHFA treatment accelerated the packing assemblies of bundles to form superbundles. Such a high packing density may contribute to a high microporosity and large specific surface area from the SWCNT superbundles, as will be described later in N_2 adsorption experiments.

Raman spectroscopy was employed to identify the formation of defects on SWCNTs after NHFA treatment. Figure 2 shows typical G- and D-bands of Raman spectra at an excitation energy of 785 nm for SWCNTs. All the samples had the maximum peak intensity near 1594 cm^{-1}, the so-called tangential mode (G-mode), which is related to the graphite E_{2g} symmetric intralayer mode, split due to the curvature of the rolled-up graphene sheet. The shoulder peak also appeared around 1566 cm^{-1}, which is a characteristic of SWCNTs. A broad band was usually observed around 1300 cm^{-1}, the so-called D-band, in multiwall CNTs and SWCNTs, which was a characteristic of amorphous carbon or defects. After NHFA treatment, the intensity of the peak around 1300 cm^{-1} and the intensity ratio of the G-band to D-band were scarcely changed compared to

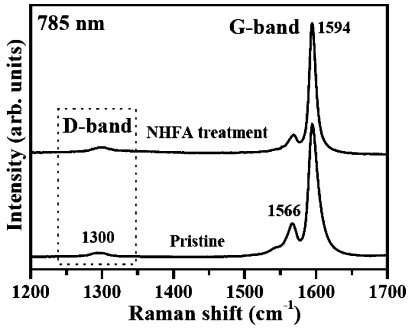

Figure 2. D- and G-bands of Raman spectra of pristine sample and NHFA-treated sample with excitation of 785 nm.

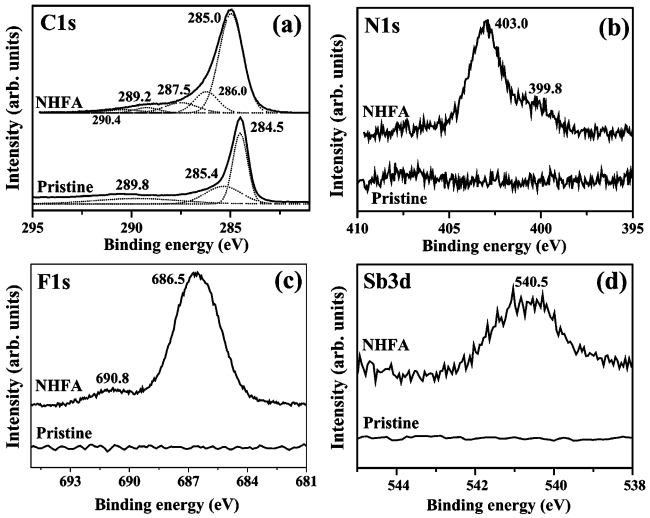

Figure 3. XPS data of (a) C ls, (b) N 1s, (c) F 1s, and (d) Sb 3d for pristine samples and samples after NHFA treatment for 24 h in 40 mmol.

those of pristine sample, indicating that defects were not formed on the tube wall by NHFA treatment. We emphasize that NHFA treatment did not change the severe structural deformation on the tube wall.

The formation mechanism of superbundles with NHFA treatment is rather subtle, particularly in organic solvents. It has been suggested that the hexafluoroantimonate ions (SbF_6^-) are intercalated to the graphite along with solvent molecules, and nitronium ions (NO_2^+) are chemisorbed to the graphite surface.[16] Here we investigated XPS spectra to see the evidence of chemisorption of NO_2^+ ions to the side wall of SWCNTs and also the intercalation of SbF_6^- into SWCNT bundles. The C 1s spectrum of the pristine SWCNTs showed three components (Figure 3a). The peak around 284.5 eV represented sp^2-hybridized carbons on the tube wall, which is comparable to the C 1s binding energy of graphite.[17] The small peak around 285.4 eV was related to sp^3-hybridized carbons that may originate from the presence of defects on the tube walls.[17] The broad peak around 289.8 eV was assigned to C−OH bonds or C−O bonds that may originate from the presence of defects on the tube wall reacting with ambient gases.[17] After NHFA treatment, these peaks were upshifted about 0.5 eV, similar to an electron acceptor behavior of adsorbates,[18] suggesting a charge transfer between nanotubes and adsorbates during NHFA treatment. This shift was completely recovered after heat treatment at 1000 °C. On the other hand, two small peaks were newly developed after NHFA treatment at 287.5 and 289.2 eV, which were assigned to C−N bonds and C−F bonds, respectively. This implies that not only the nitronium ions but also

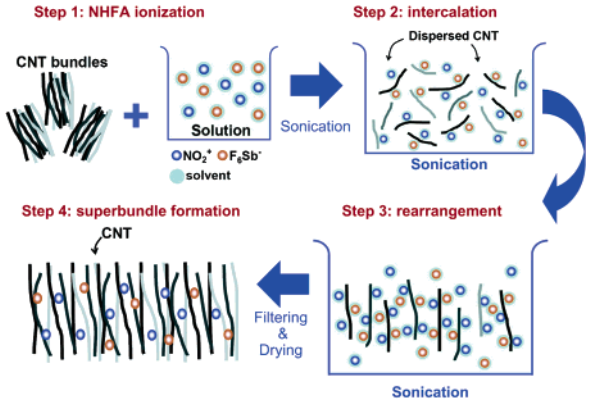

Figure 4. Schematic diagram for formation of superbundles by NHFA treatment.

the counterions (SbF_6^-) were chemisorbed on the nanotube walls. These peaks again disappeared after heat treatment. From N 1s spectra (Figure 3b), we observed the N−O related peak near 403 eV,[19] which is the evidence of NO_2^+ ion intercalation. We also observed the C−N related peak near 399.8 eV.[19] This strongly indicates that the nitrogen atom of NO_2^+ ions was chemisorbed partially with nanotube walls, while most NO_2^+ ions were simply intercalated between nanotubes in the bundles that could be easily removed during heat treatment, consistent with no appreciable change in the C−O peak of C 1s spectra. It is worth mentioning that the nanotubes with chemically bonded oxygen atoms of NO_2^+ ions were disintegrated similarly to the oxidative etching, and further filtrated during the filtering procedure. The F 1s XPS spectrum of the NHFA-treated SWCNTs revealed two main peaks (Figure 3c). The large peak at 686.5 eV originated from the ionic C−F bonds of the intercalated SbF_6^- on the tube wall.[20] The small peak around 690.8 eV represented the covalent C−F bonds on the tube wall,[20] which was consistent with the small peak near 289.2 eV in the C 1s spectrum. The SbO_x-related peak was also observed near 540.5 eV in the NHFA-treated sample due to an intercalation of SbF_6^-.[21] These intercalants were again completely removed after thermal annealing at 1000 °C.

The XPS data demonstrate that both anions and cations are intercalated into bundles to form covalent bonds with nanotube walls. We emphasize that the superbundles were not formed without intercalants, i.e., an intercalant-induced rearrangement of nanotubes. It has been reported that the rearrangement of SWCNTs, which is similar to our case, occurs by the intercalation of sulfuric acids.[22,23] In superacid (100% sulfuric acid), the SWCNTs formed charge-transfer complexes in which positively charged individual nanotubes were surrounded by sulfuric acid anions.[23] The SWCNT/acid charge-transfer complexes easily formed ordered ropes through the rearrangement of nanotubes.[23] Here we propose schematically a concerted pathway of superbundle formation induced by the NHFA treatment (Figure 4). NHFA was ionized in TMS/chloroform solvent into nitronium ions and hexafluoroantimonate ions as follows (step 1):

$$NO_2SbF_6 \rightarrow NO_2^+ + SbF_6^-$$

SbF_6^- ions are first inserted along with solvent molecules into SWCNT bundles, where the debundling of nanotubes is enhanced by the charge transfer, similar to the sulfuric acids.[23] This provides more room for NO_2^+ ions to intercalate into the nanotube bundles, expanding the interlayer distances in bundles, similar to the graphite (step 2).[16] The NO_2^+ ions capture the available π-electrons in the graphite, enhancing the binding energy with the graphite surface. Since π-electrons of the SWCNT surface are similar to those of graphite, we expect that the NO_2^+ ions can attack π-electrons on the nanotube surface and thus provoke stable adsorption. The binding of NO_2^+ ions with nanotubes could be promoted by an assistance of strain effect present in the tube wall. This weakens the tube−tube interactions. The nanotube dispersion into individual nanotubes or small bundles is enhanced by the physical excitation with sonication. The XPS also confirms that a considerable number of the SbF_6^- ions are chemisorbed. The individual nanotubes or small bundles become more floppy such that these nanotubes are rearranged more easily into superbundles via the intercalant interaction during flotation in the solvent (step 3). As the solvent molecules are extracted by filtering and drying processes, the rearranged SWCNTs are densely packed, resulting in the formation of superbundles (step 4). The rearrangement of individual nanotubes into bundle occurs inside an individual superbundle. The formed superbundles are randomly entangled in each other, as shown in Figure 1. We emphasize that the rearrangement of SWCNTs can occur in solution by forming an SWCNT−intercalant charge complex.

The formation of superbundles gives rise to significantly altering the pore structures of nanotubes. We measured N_2 adsorption isotherms at 77 K to obtain quantitative evidence of the pore structure changes. Figure 5a presents N_2 adsorption isotherms of the pristine and NHFA-treated SWCNTs. The pristine SWCNTs show type II adsorption isotherm according to IUPAC classification by revealing a gradual uptake of N_2 at the medium relative pressure (P/P_0) and also a predominant adsorption of N_2 at high pressure, which is related to the multilayer adsorption on the external surface and macropores. After NHFA treatment, N_2 adsorption isotherm transforms to type I with a steep uptake at low pressure and a long plateau at medium pressure, although it exhibits a slight adsorption uptake at high pressure. This is associated with the presence of uniform microporosity and a small amount of external surfaces due to the large bundle size of the NHFA-treated SWCNTs. The hysteresis loop is of type H4, which is generally given by slit-shaped pores.[24] The hysteresis loop of type H4 originates mainly from the micropore distribution of porous materials. Furthermore, the NHFA-treated SWCNTs exhibit an enhanced adsorption uptake of N_2 below $P/P_0 = 0.1$, indicating further development of micropores that are newly produced by the superbundle formation of SWCNTs. The inset in Figure 5a shows N_2 adsorption isotherms in a logarithmic scale to show the detailed adsorption behavior of N_2 at low pressure. The NHFA-treated SWCNT superbundles show a much higher adsorption capacity of N_2 at low pressure compared with the pristine SWCNTs, indicating enhanced adsorbent−adsorbate interactions due to development of microporosity.

Figure 5b shows high-resolution α_s-plots for N_2 adsorption isotherms of the pristine and NHFA-treated SWCNTs at 77 K. The subtracting pore effect (SPE) method using an α_s-plot has been used as an effective method for porosity evaluation. The slopes of solid and dotted lines give information about the total and external surface areas, respectively. The micropore volume was calculated from the ordinate intercept of the dotted line. The upward deviation due to the monolayer adsorption on the micropore walls is observed at the low α_s-region (>0.1). The NHFA-treated SWCNTs show an enhanced upward deviation due to the developed microporosity. The pore structure parameters of the samples obtained by the SPE method using the high-resolution α_s-plots are summarized in Table 1. The mesopore volume was obtained by subtracting the micropore volume from

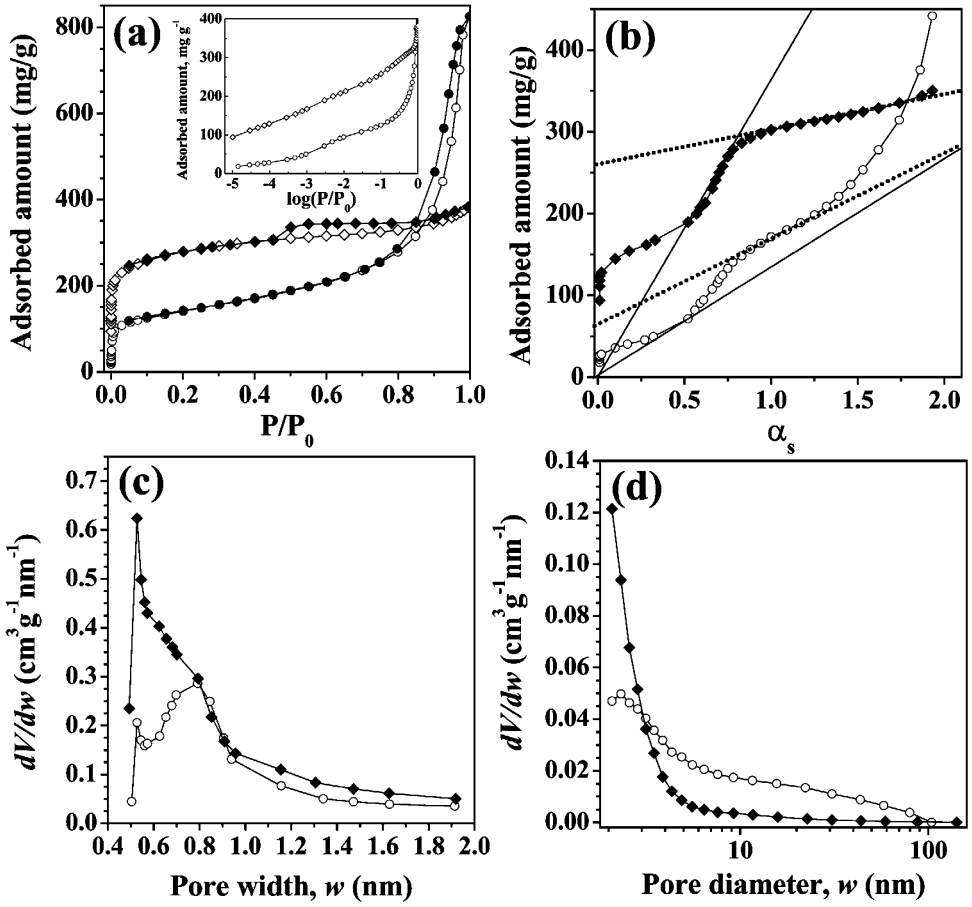

Figure 5. (a) N_2 adsorption isotherms (77 K) of SWCNTs. The open and filled symbols indicate adsorption and desorption branches, respectively. The insert shows N_2 adsorption isotherms in logarithmic scale. (b) α_s-plots of the N_2 adsorption isotherms of SWCNTs. (c) Micropore size distributions determined by HK method. (d) Mesopore size distributions determined by BJH method. Pristine SWCNTs: ○, adsorption; ●, desorption. NHFA-treated SWCNTs: ◇, adsorption; ◆, desorption.

TABLE 1: Pore Structure Parameters of SWCNTs Determined by BET and SPE Methods

	BET	SPE						
samples	surf. area (m^2 g^{-1})	total surf. area (m^2 g^{-1})	micropore surf. area (m^2 g^{-1})	external surf. area (m^2 g^{-1})	total pore vol (mL g^{-1})	micropore vol (mL g^{-1})	mesopore vol (mL g^{-1})	micropore vol percent (%)
pristine SWNTs	394	287	100	187	0.96	0.10	0.86	10
NHFA-treated SWNTs	817	778	693	85	0.46	0.32	0.14	70

the total pore volume, which was determined from the adsorbed N_2 amount at $P/P_0 = 0.98$. The NHFA treatment remarkably increased the total surface area and micropore volume. In particular, the micropore surface area and micropore volume increased about 7 and 3 times, respectively, after NHFA treatment, whereas the mesopore volume dramatically decreased from 0.86 to 0.14 mL g^{-1}. The NHFA treatment was efficient for developing the microporosity of SWCNT superbundles. This analysis of pore structures provides quantitative information for the bundling of SWCNTs. Such an enhanced microporosity after NHFA treatment is contributed from the increment of interstitial space through the formation of superbundles. Furthermore, the micropore volume percent remarkably increased from 10 to 70% after NHFA treatment, which is associated with a transformation of pore structures from macropores to micropores. It is important to note that the external surface area decreased from 187 to 85 m^2 g^{-1} as a consequence of the NHFA treatment, indicating the enlarged bundle size.

We also used the Horvath−Kawazoe (HK) method to obtain the micropore size distribution, assuming slit-shaped pores. Figure 5c shows the micropore size distribution determined by the HK method. The pore size distribution (PSD) of the pristine SWCNTs is mainly in the range 0.5−1.0 nm, with a shoulder in the range 1.0−2.0 nm. After NHFA treatment, the peak intensity from 0.5 to 1.0 nm increased considerably, suggesting that the NHFA treatment developed a narrow microporosity due to an increase of interstitial sites with the maximum size of 0.5 nm by the enlarged bundle size. The mesopore size distributions were calculated by the BJH method, assuming cylindrical-shaped pores (Figure 5d). The pristine SWCNTs show a broad PSD of up to 100 nm. On the other hand, the NHFA-treated SWCNTs did not show mesopores wider than 10 nm, suggesting that the interbundle distance decreased through the formation of the superbundle. The PSDs obtained from both HK and BJH methods clearly demonstrated that the PSDs of SWCNT superbundles were shifted to the smaller pore sizes. Thus N_2 adsorption is able to provide conclusive evidence of superbundle formation, which is consistent with the morphological observations from FESEM.

Conclusion

In summary, our approach has shown a simple and easily scalable method for the formation of superbundles. Most SWCNT bundles with the NHFA treatment were enlarged by about 10 times compared to those of the pristine sample. The formation of SWCNT superbundles induced by intercalants during the NHFA treatment increased the total surface area, micropore surface area, and micropore volume, while the external surface area, mesopore surface area, and pore width were decreased. This development of microporosity resulted from the enhanced interstitial sites in the SWCNT superbundles. We propose a concerted pathway for the structural formation of the SWCNT superbundles induced by intercalants during NHFA treatment based on our experimental observations.

Acknowledgment. This project was supported by the Ministry of Science and Technology through the National Research Laboratory program, in part by the Center for Nanotubes and Nanostructured Composites at Sungkyunkwan University, and in part by the Korea Energy Management Corporation (2004-N-HY12-P-02-0-000).

References and Notes

(1) Lee, S. M.; Park, K. S.; Choi, Y. C.; Park, Y. S.; Bok, J. M.; Bae, D. J.; Nahm, K. S.; Choi, Y. G.; Yu, S. C.; Kim, N. G.; Frauenheim, T.; Lee, Y. H. *Synth. Met.* **2000**, *113*, 209.

(2) Lueking, A.; Yang, R. T. *AICHE J.* **2003**, *49*, 1556.

(3) Wang, C.; Waje, M.; Wang, X.; Tang, J. M.; Haddon, R. C.; Yan, Y. *Nano Lett.* **2004**, *4*, 345.

(4) Gao, B.; Bower, C.; Lorentzen, J. D.; Fleming, L.; Kleinhammes, A.; Tang, X. P.; McNeil, L. E.; Wu, Y.; Zhou, O. *Chem. Phys. Lett.* **2000**, *327*, 69.

(5) An, K. H.; Kim, W. S.; Park, Y. S.; Choi, Y. C.; Lee, S. M.; Chung, D. C.; Bae, D. J.; Lim, S. C.; Lee, Y. H. *Adv. Mater.* **2001**, *13*, 497.

(6) An, K. H.; Jeon, K. K.; Heo, J. K.; Lim, S. C.; Bae, D. J.; Lee, Y. H. *J. Electrochem. Soc.* **2002**, *149*, A1058.

(7) Dai, G.-P.; Liu, C.; Liu, M.; Wang, M.-Z.; Cheng, H.-M. *Nano Lett.* **2002**, *2*, 503.

(8) Zhu, H.; Cao, A.; Li, X.; Xu, C.; Mao, Z.; Ruan, D.; Liang, J.; Wu, D. *Appl. Surf. Sci.* **2001**, *178*, 50.

(9) Cao, A.; Zhu, H.; Zhang, X.; Li, X.; Ruan, D.; Xu, C.; Wei, B.; Liang, J.; Wu, D. *Chem. Phys. Lett.* **2001**, *20*, 510.

(10) Lee, Y. H.; An, K. H.; Lim, S. C.; Kim, W. S.; Jeong, H. J.; Doh, C.-H.; Moon, S.-I. *New Diamond Front. Carbon Technol.* **2002**, *12*, 209.

(11) Yang, C. M.; Kaneko, K.; Yudasaka, M.; Iijima, S. *Nano Lett.* **2002**, *2*, 385.

(12) Moon, J.-M.; An, K. H.; Lee, Y. H.; Park, Y. S.; Bae, D. J.; Park, G.-S. *J. Phys. Chem. B* **2001**, *105*, 5677.

(13) Shelimov, K. B.; Esenaliev, R. O.; Rinzer, A. G.; Huffman, C. B.; Smalley, R. E. *Chem. Phys. Lett.* **1998**, *282*, 429.

(14) Gennett, T.; Dillon, A. C.; Alleman, J. L.; Jones, K. M.; Haesoon, F. S.; Heben, M. J. *Chem. Mater.* **2000**, *12*, 599.

(15) Ausman, K. D.; Pinger, R.; Lourie, O.; Ruoff, R. S.; Korobov, M. *J. Phys. Chem. B* **2000**, *104*, 8911.

(16) Forsman, W. C.; Mertwoy, H. E. *Synth. Met.* **1980**, *2*, 171.

(17) An, K. H.; Jeong, G. H.; Jeon, K. G.; Bae, D. J.; Jo, C.; Yang, C. W.; Park, C.-Y.; Lee, Y. H.; Lee, Y. S.; Chung, Y. S. S. *Appl. Phys. Lett.* **2002**, *80*, 4235.

(18) Dettlaff-Weglikowska, U.; Benoit, J.-M.; Chiu, P.-W.; Graupner, R.; Lebedkin, S.; Roth, S. *Curr. Appl. Phys.* **2002**, *2*, 497.

(19) Biniak, S.; Szymanski, G.; Siedlewski, J.; Swiatkowski, A. *Carbon* **1997**, *35*, 1799.

(20) Hayashi, T. *Nano Lett.* **2004**, *4*, 1001.

(21) Zeng, D. W.; Zhu, B. L.; Xie, C. S.; Song, W. L.; Wang, A. H. *Mater. Sci. Eng., A* **2004**, *366*, 332.

(22) Ericson, L. M.; et al. *Science* **2004**, *305*, 1447.

(23) Davis, V. A.; et al. *Macromolecules* **2004**, *37*, 154.

(24) Rouquerol, F.; Rouquerol, J.; Sing, K. *Adsorption by Powders and Porous Solids*; Academic Press: London, 1999.